

## Excitation functions for the helium-ion-induced fission of holmium and erbium

R. H. Iyer, A. K. Pandey, P. C. Kalsi, and R. C. Sharma

*Radiochemistry Division, Bhabha Atomic Research Centre, Trombay, Bombay-400085, India*

(Received 18 December 1990)

Excitation functions for the helium-ion-induced fission of holmium ( $Z=67$ ) and erbium ( $Z=68$ ) in the energy range 34–70 MeV were measured using lexan polycarbonate plastic as the fission fragment track detector. By analyzing the data in terms of the statistical model expression for  $\Gamma_f/\Gamma_n$ , the ratio of the fission width to neutron emission width, the fission barriers of the compound nuclei  $^{169}\text{Tm}$  and  $^{171,3}\text{Yb}$  were determined to be  $29.8\pm 3$  and  $27.8\pm 3$  MeV, respectively. The corresponding values for the fission level density parameter were found to be  $a_f = A/12$  and  $A/13$ , respectively. The uncertainties shown in the fission barriers allow for inclusion of other values derived from reasonable upper and lower limits of  $a_f$  values of  $A/8$  to  $A/20$ . The measured fission barriers compare very well with the shell-corrected liquid-drop barriers of Myers and Swiatecki. The present measurements extend the range of low- $Z$  elements which are away from the closed-shell region and which are studied at these medium energies. The results are compared with similar data available in the literature which bring out some interesting correlations and trends in the fission properties, viz., fission barriers and level density parameters of low- $Z$  elements.

### I. INTRODUCTION

Although rather extensive data on the fission properties of heavy elements ( $Z \geq 90$ ) are available in the literature [1], those on lighter elements ( $Z \leq 80$ ) are very limited. This is because even at excitation energies well above the fission threshold, the fission cross sections of lighter elements are extremely small, of the order of nanobarns ( $10^{-33} \text{ cm}^2$ ) which puts extremely stringent requirements on target purity with regard to heavy element contamination and makes experimental measurements somewhat difficult. A further requirement is that the measurement methods should not only be extremely sensitive but also highly discriminating. Nevertheless, fission studies on low- $Z$  elements induced by intermediate energy ( $\lesssim 100$  MeV) charged particles provide excellent opportunities for determining important nuclear parameters such as fission barriers ( $E_f$ ), level density parameters for neutron emission ( $a_n$ ) and fission ( $a_f$ ), influence of shell effects, etc., by analyzing the fission excitation functions and for comparing these parameters with predictions of theoretical models [2].

Early radiochemical work of Fairhall and co-workers on the charge-particle-induced fission of lighter elements in the gold-bismuth region clearly demonstrated that low- $Z$  element fission is predominantly symmetric and the fission cross sections vary very rapidly with excitation energy [3,4]. Considering the limitations of radiochemical techniques in the measurements of low-fission cross sections, semiconductor detectors were used very effectively in the He-ion-induced fission excitation functions of Bi, Pb, Ti, and Au [5]—the lowest total fission cross sections measured being of the order of a microbarn ( $10^{-30} \text{ cm}^2$ ).

Using the solid-state nuclear track detector (SSNTD) mica for detection of fission fragments [6], Burnett *et al.*

[7] were able to measure fission cross sections as low as  $10^{-35} \text{ cm}^2$  in one of the most extensive and careful measurements of the He-ion-induced fission excitation function of Au and determined the fission barrier of  $\text{Tl}^{201}$ . The extreme sensitivity and selectivity of SSNTDs for fission fragment detection was further used to advantage by Raisbeck and Cobble [8], who extended these studies to some of the lightest elements such as rhenium ( $Z=75$ ), lutetium ( $Z=71$ ), and thulium ( $Z=69$ ). The reason for choosing rare earths was that they are in the region of deformed nuclei away from closed-shell configurations and it was of interest to see whether the ground-state deformation has any observable effect on the fission barrier and the level density parameters. This work [8] provided some excellent systematics on fission barriers and level density parameters over a wide range of  $Z$ . In particular, it showed (a) good agreement between the measured fission barriers and those predicted by a semiempirical mass formulation based on a charged liquid drop [9], (b) that the  $a_f/a_n$  ratios tend to decrease with mass number of the compound nucleus and are significantly lower than the ratios found for nuclides near the closed shells [7,10], which suggested that as one moves away from closed-shell nuclei, the ground state and saddle point have a similar level structure and  $a_f$  and  $a_n$  tend to become equal [11]. (c) While the “best fits” to the experimental  $\Gamma_f/\Gamma_n$  ratio (the ratio of fission width to neutron emission width equated to  $\sigma_f/\sigma_R$  the ratio of fission cross section to total reaction cross section) suggested a value of  $a_f = A/8$  for both Lu and Tm that for natural Re was an anomalously low value of  $A/20$ . Since Burnett *et al.* [7] found a value of  $a_f \approx A/11$  for the fission of gold, the anomalously low value of  $A/20$  for Re could be attributed to the use of mixed isotopes. However, the later work of Brodzinski and Cobble [12] on the He-induced fission of natural iridium ( $Z=77$ ) which lies

between Re and Au and which has a mixture of two isotopes of nearly the same abundance as natural Re gave a value of  $a_f = A/10$ . More recently, using glass detectors, Kuvatov *et al.* [13] reported results of fission cross sections and fragment angular anisotropies in the 38 MeV He-ion-induced fission of several nuclei in the region  $Z=73-83$  and have made some interesting observations on the systematics of  $a_f$  and  $a_n$  in the low- $Z$  element region.

As part of a long-range program of work on the fission properties of low- $Z$  ( $Z < 80$ ) elements, we report in this paper the results of our work on the fission excitation functions of natural erbium ( $Z=68$ ) and holmium ( $Z=67$ ) induced by He-ions in the energy range of 34–70 MeV using the Variable Energy Cyclotron at Calcutta. We have extended the measurements of Raisbeck and Cobble [8] to still lower rare earths, viz., erbium ( $Z=68$ ) and holmium ( $Z=67$ ) using identical measurement techniques. Since Lu, Tm, and Ho are monoisotopic, natural Er was used specifically to look for any unusual effects in the fission barrier or level density parameter. The excitation functions were analyzed in terms of  $\Gamma_f/\Gamma_n$ . Our results on fission barriers and level density parameters are compared with other available data on low- $Z$  systems. Some preliminary results of this work have been reported previously [14,15].

## II. EXPERIMENTAL PROCEDURES

One of the most challenging problems with regard to these experiments was to ensure stringent purity of the holmium and erbium targets as well as the silver backing foils used. Since rare-earth elements are commonly associated with thorium and uranium, both of which have fission cross sections about  $10^9$  greater than those of the elements under study, it was essential that the level of these contaminants be less than a few parts per billion (ppb). "Spec pure" rare-earth oxides with certificate of analysis were obtained from M/s. Johnson Mathey Chemicals Ltd., England. Even though the levels of U and Th in the oxides were certified to be "below detection limit" of 1 part per million (ppm), about a gram each of the oxides of Ho and Er were further purified by a series of anion exchange separations using both HCl and HNO<sub>3</sub> media [16]. The chloride columns removed uranium while the nitrate columns removed thorium completely. The rare earths were finally precipitated as the oxalates and ignited at 800°C to give the oxide powder. Extreme care was taken to see that no external contamination occurred during the purification steps. Only high-purity reagents, polythene wares, and quartz apparatus were used.

Silver backing foils of 10–12 mg/cm<sup>2</sup> thickness were prepared by vacuum evaporation of 99.9999% silver beads (obtained from United Mineral and Chemical Corporation, New York) onto a lexan polycarbonate film [17], which was subsequently dissolved in methylene dichloride. Thin, uniform deposits of rare-earth oxides of 1–2 mg/cm<sup>2</sup> thickness on the silver foils were made initially by an electrophoresis technique [18] using a Teflon cell. A slurry of rare-earth oxides in distilled acetone was

taken in the cell and a dc voltage of 400–500 V was used across two thick copper electrodes placed in the cell for a few seconds. The rare-earth oxides got deposited on the silver foil kept in contact with the copper electrodes. In a later modification, the slurry containing a few mg of the fine oxide powder in distilled acetone was gradually allowed to settle on the pure silver foil placed inside the Teflon cell. The acetone was gently sucked out with a syringe leaving a thin and uniform coating of the oxide film, the thickness of which was determined by weighing in a microbalance. The absence of any detectable heavy element contamination in the purified rare-earth oxides and the blank silver backing foils was checked by irradiating the samples with reactor neutrons in the core of APSARA swimming pool reactor and looking for fission events in lexan track detector strips [6] placed in contact with the samples. The maximum heavy element contamination was estimated to be no more than 3–5 parts per billion (ppb). The irradiation assembly used for the measurement of fission cross sections was almost identical to the one used by Raisbeck and Cobble [8] in their work. Fission fragments recoiling out of the thin target in the backward direction with respect to the incident beam of alpha particles were recorded using a cylindrical lexan plastic track detector of 2.5 cm height and 1.6 cm diameter mounted inside the target assembly. This arrangement provided both the sensitivity and the necessary discrimination against nonfission nuclear reactions. It also allowed fragments recoiling in the backward hemisphere over the laboratory angles 90°–165° to be detected. The He-ion beams of different energies from the 88" Variable Energy Cyclotron at Calcutta were collimated through two stainless-steel collimators, (a 3 mm diameter followed by a 5 mm diameter) before striking the target. The target holder acted as a Faraday cup. Total integrated beam currents of the order of 1–2  $\mu$ Ah were used in each experiment. A few initial runs were carried out on the targets and blank silver foils with 30 and 35 MeV He-ions to verify their purity. Any fission event recorded on the detector was attributed to be arising from heavy elements and was taken into account in calculating the fission cross sections.

After irradiation, the lexan detector foils were removed and etched in 6N NaOH at 60°C for 1 h. Horizontal strips of the detector at a fixed distance from the base which corresponded to a fixed angle of emission of the fragment with respect to the beam were scanned under an optical microscope [19] (see Fig. 1). From the measured track density (number of tracks/cm<sup>2</sup>) at various laboratory angles the fragment angular distribution could also be obtained [19]. However, in the present measurements, this was done only at the highest bombarding energies where because of the higher  $\sigma_f$ , good track counting statistics could be obtained. In most other cases, a reasonably large area was scanned to get good statistics in counting.

A photomicrograph of the oriented fission tracks from the fission of holmium at 65 MeV is shown in Fig. 2. The absolute fission cross sections were calculated by comparing the number of tracks in a specified area (observation solid angle) in the detector from the sample (holmium

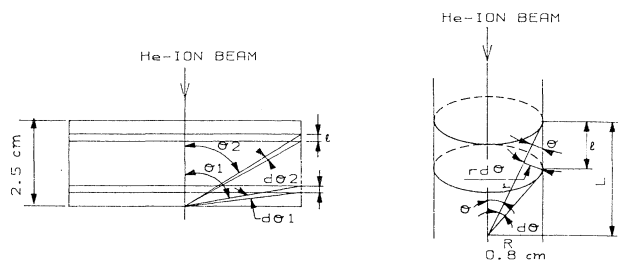


FIG. 1 Schematic diagram showing the track registration geometry. The right-hand diagram shows the position of the cylindrical lexan detector inside the target holder during irradiation. The left-hand diagram shows the unfolded lexan foil as fixed on the microscope slide. Each horizontal strip  $l$  scanned corresponds to a definite angle which the fission fragments make with the He-ion beam.

and erbium in this case) with the number of tracks in the same area from a standard, irradiated under the same experimental conditions. In most of the measurements, the track densities at observation solid angles corresponding to laboratory angles from  $122^\circ$  to  $148^\circ$  were compared in the samples and standards [this corresponded to the detector area between 5 and 13 mm from the base of the detector strip (see Fig. 1)]. In these experiments, we used both lutetium and gold as standards whose absolute fission cross sections as a function of He-ion energy are known [7,8]. Once the fission cross section at one energy is determined, it serves as a normalizing point and cross sections at any other energy can be calculated by comparing the track densities (number of tracks per  $\text{cm}^2$  at a specified area) and taking into account the target thickness and beam current.

Thus

$$\sigma_s = \sigma_{\text{ref}} \frac{D_s}{D_{\text{ref}}} \frac{Q_{\text{ref}}}{Q_s} \frac{n_{\text{ref}}}{n_s}, \quad (1)$$

where  $\sigma$  is the cross section,  $D$  the track density (number of tracks /  $\text{cm}^2$ ),  $Q$  the number of  $\alpha$  particles, and  $n$  the number of target atoms /  $\text{cm}^2$ .

The subscripts  $s$  and  $\text{ref}$  refer to sample and reference standard, respectively.



FIG. 2. Photomicrograph of the oriented fission fragment tracks in lexan from the 65 MeV He-ion-induced fission of  $^{165}\text{Ho}$ .

It may be noted that, because of the low cross sections involved (see Tables I and II) and the relatively low track densities, this approach of comparative measurement was considered more desirable rather than measuring the differential cross sections and integrating over the entire solid angle to get the absolute fission cross sections.

### III. EXPERIMENTAL RESULTS

The measured total fission cross sections for the helium-ion-induced fission of  $^{165}\text{Ho}$  and natural  $^{167.3}\text{Er}$  (0.136%  $^{162}\text{Er}$ , 1.56%  $^{164}\text{Er}$ , 33.41%  $^{166}\text{Er}$ , 22.94%  $^{167}\text{Er}$ , 27.07%  $^{168}\text{Er}$ , and 14.88%  $^{170}\text{Er}$ ) are given in Tables I and II and shown in Fig. 3. The excitation energies were calculated by assuming full momentum transfer and using the mass tables of Myers and Swiatecki [9]. A  $Q$  value of  $-1.137$  MeV for the  $^{165}\text{Ho} + ^4\text{He}$  reaction and a weighted average  $Q$  value of  $-1.4$  MeV for the  $^{167.3}\text{Er}(\text{nat}) + ^4\text{He}$  reaction was used.

The errors quoted in the measured cross sections are only statistical errors involved in track counting. The other sources of errors include those arising from varia-

TABLE I. Experimental fission cross sections for holmium  $^{165}\text{Ho} + ^4_2\text{He} \rightarrow ^{169}\text{Tm}$ .

$^4\text{He}$ ion energy (MeV)	Excitation energy (MeV)	Measured fission cross section $\sigma_f$ ( $\text{cm}^2$ )	Calculated reaction cross section $\sigma_R$ ( $\text{cm}^2$ )	$\Gamma_f/\Gamma_n \approx (\sigma_f/\sigma_R)$
70.0	67.2	$(2.75 \pm 0.09) \times 10^{-30}$	$2.185 \times 10^{-24}$	$1.259 \times 10^{-6}$
65.0	62.3	$(1.50 \pm 0.16) \times 10^{-30}$	$2.146 \times 10^{-24}$	$6.990 \times 10^{-7}$
60.0	57.4	$(8.42 \pm 0.44) \times 10^{-31}$	$2.098 \times 10^{-24}$	$4.013 \times 10^{-7}$
55.0	52.6	$(2.29 \pm 0.39) \times 10^{-31}$	$2.038 \times 10^{-24}$	$1.124 \times 10^{-7}$
50.0	47.7	$(8.90 \pm 0.78) \times 10^{-32}$	$1.962 \times 10^{-24}$	$4.536 \times 10^{-8}$
45.3	43.1	$(5.80 \pm 0.80) \times 10^{-33}$	$1.864 \times 10^{-24}$	$3.112 \times 10^{-9}$
45.0	42.8	$(2.50 \pm 0.90) \times 10^{-33}$ <sup>a</sup>	$1.864 \times 10^{-24}$	$1.341 \times 10^{-9}$
40.0	37.9	$(0.71 \pm 0.30) \times 10^{-33}$	$1.735 \times 10^{-24}$	$4.092 \times 10^{-10}$

<sup>a</sup>This value was not included in the barrier calculations because the blank corrections were large.

TABLE II. Experimental fission cross sections for erbium (natural)  $^{167,3}_{68}\text{Er} + {}^4_2\text{He} \rightarrow {}^{171,3}_{70}\text{Yb}$ .

${}^4\text{He}$ ion energy (MeV)	"Average" excitation energy (MeV)	Measured fission cross section $\sigma_f$ ( $\text{cm}^2$ )	Calculated reaction cross section $\sigma_R$ ( $\text{cm}^2$ )	$\Gamma_f/\Gamma_n \approx (\sigma_f/\sigma_R)$
65.0	62.1	$(2.40 \pm 0.07) \times 10^{-30}$	$2.149 \times 10^{-24}$	$1.117 \times 10^{-6}$
60.0	57.2	$(1.25 \pm 0.05) \times 10^{-30}$	$2.089 \times 10^{-24}$	$5.984 \times 10^{-7}$
55.0	52.3	$(5.30 \pm 0.22) \times 10^{-31}$	$2.035 \times 10^{-24}$	$2.604 \times 10^{-7}$
50.0	47.4	$(2.03 \pm 0.18) \times 10^{-31}$	$1.955 \times 10^{-24}$	$1.038 \times 10^{-7}$
45.3	42.8	$(3.80 \pm 0.20) \times 10^{-32}$	$1.852 \times 10^{-24}$	$2.052 \times 10^{-8}$
45.0	42.5	$(3.69 \pm 0.37) \times 10^{-32}$	$1.852 \times 10^{-24}$	$1.992 \times 10^{-8}$
40.0	37.6	$(4.48 \pm 1.02) \times 10^{-33}$	$1.735 \times 10^{-24}$	$2.582 \times 10^{-9}$
34.3	32.1	$\leq 7 \times 10^{-33}{}^a$	$1.535 \times 10^{-24}$	$\leq 4.56 \times 10^{-9}$

<sup>a</sup>This value was not included in barrier calculations because the blank corrections were large.

tions in target thickness, heavy element contamination, integrated beam current, variation of track densities along the length of the detector film (see Fig. 1) due to the He beam being slightly off center, assumptions regarding geometry, uncertainty in the reference cross sections, etc. The overall accuracy of the results is estimated to be about 20% at all He-ion energies above 45 MeV. At the lower energies the overall accuracy of the results is estimated to be about 50%.

#### IV. DISCUSSION

One of the objectives of the present research was to examine the trend of fission barriers and level density parameters in compound nuclei lighter than those for which experimental data have been reported [8] and thereby to extend the available systematics of these nuclear param-

eters to lower values of  $Z$ . The most common method of analyzing fission excitation functions of low- $Z$  elements is by using a statistical model expression suggested by Vandebosch and Huizenga [2]. The steep excitation functions (see Fig. 3) suggest that the measured fission cross sections are mostly due to first change fission. Therefore, the fission width  $\Gamma_f$  is very nearly equal to the fission cross section  $\sigma_f$ . Charged-particle emission can be ignored at these moderate energies and therefore the neutron emission width  $\Gamma_n$  can be approximated with the total reaction cross section,  $\sigma_R$ . Thus

$$\Gamma_f/\Gamma_n \approx \sigma_f/\sigma_R. \quad (2)$$

The experimental  $\Gamma_f/\Gamma_n$  values as a function of excitation energy for erbium and holmium are shown in Fig. 4.

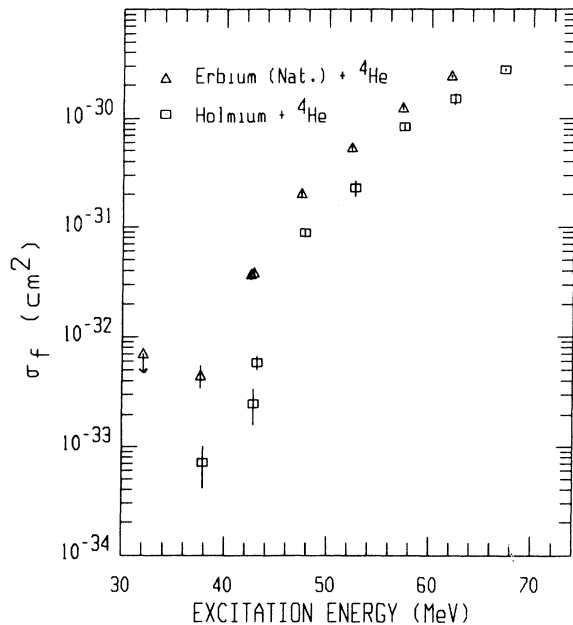


FIG. 3. Measured fission excitation functions in the He-ion-induced fission of holmium and natural erbium.

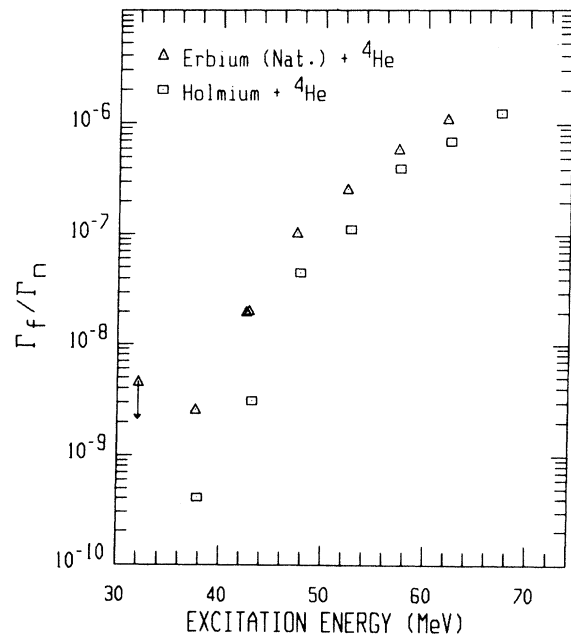


FIG. 4. Plot of the fission to neutron emission width ratios vs excitation energy for the He-ion-induced fission of holmium and natural erbium.

The total reaction cross sections were calculated according to the optical model of Huizenga and Igo [20] using the ALICE computer code [21]. The experimental  $\Gamma_f/\Gamma_n$  values were analyzed using the theoretical expression

$$\Gamma_f/\Gamma_n = K_0 \frac{a_n [2a_f^{1/2}(E - E_f)^{1/2} - 1]}{4A^{2/3}a_f(E - Bn)} \times \exp[2a_f^{1/2}(E - E_f)^{1/2} - 2a_n^{1/2}(E - Bn)^{1/2}], \quad (3)$$

where  $a_n$  and  $a_f$  are the level density parameters for neutron emission and fission, respectively,  $E$  is the excitation energy,  $E_f$  is the fission barrier,  $B_n$  is the neutron binding energy,  $A$  is the mass number of the compound nucleus, and  $K_0$  is a constant taken as 10.7 MeV ( $K_0 = \hbar^2/gmr_0^2$ ). ( $K_0 = \hbar/gmr_0^2$ , where  $g=2$  corresponding to the spin states of the neutron,  $m$  is the mass of the neutron, and  $r_0$  is the radius parameter taken as  $1.4 \times 10^{-13}$  cm.) It is easy to realize that an expression of such flexibility as Eq. (3) will give good fits to the experimental  $\Gamma_f/\Gamma_n$  data for various “sets” of the three adjustable parameters  $a_n$ ,  $a_f$ , and  $E_f$  unless the experimental data are extensive in which case one can expect to get unique values for these parameters.

In the present work we used a least-squares-fitting procedure in which instead of “floating” all the three parameters we allowed (a) values of  $a_f$ , to vary between  $A/8$  and  $A/20$  (reasonable upper and lower limits), (b) allowed the values of  $a_f/a_n$  to vary from 1.00 to 1.35 in increments of 0.01, and (c) allowed  $E_f$  value to vary between 20 and 35 MeV, in increments of 0.1 MeV. By this procedure, the  $E_f$  values were calculated and the “best” values were selected on the basis of the sum of the squares of the deviation ( $\psi^2$ ) which gives a measure of the “goodness of fit.” The results of the least-squares-fitting procedure are listed in Tables III and IV.

It is instructive to compare these results with similar data available in the literature [5,7,8,12] and examine the trends in the values of  $E_f$ ,  $a_f$ ,  $a_n$ , and  $a_f/a_n$  particularly in low- $Z$  ( $Z < 80$ ) systems. In making these comparisons, it should be noted that in the present work we have used the simplest form of the statistical model expression [Eq. (3)] neglecting several factors which are believed to be small, like angular momentum brought in by alpha particles, barrier penetration [7] pairing and shell corrections to the neutron binding energies [5], etc.

As mentioned earlier, because of the flexibility of the theoretical expression for  $\Gamma_f/\Gamma_n$  as given in Eq. (3), as also indicated by the results of others [5,7,8] and confirmed by the present work, it is possible to get sufficiently good fits to the experimental  $\Gamma_f/\Gamma_n$  ratio with different “sets” of parameters:  $a_f$ ,  $a_n$ , and  $E_f$ . Therefore, rather than assigning “unique” values of  $E_f$ ,  $a_f$ , and  $a_n$ , it seems more appropriate to choose the values which lie in the neighborhood of the “best fits” as judged from the sum of squares of the deviations [7]. Thus from Tables III and IV, we make the following observations:

(a) For  $^{171.3}_{70}\text{Yb}$ ,  $E_f$  lies in the vicinity of 25–30.8 MeV, with the corresponding ( $a_f$ ,  $a_n$ ) values varying between (21.4, 20.8)  $\text{MeV}^{-1}$  and (8.6, 8.6)  $\text{MeV}^{-1}$ , and  $a_f/a_n$  varying between 1.03 and 1.00.

(b) For  $^{169}_{69}\text{Tm}$ ,  $E_f$  lies in the vicinity of 27.4–32.6 MeV, with the corresponding ( $a_f$ ,  $a_n$ ) values varying between (21.1, 19.9)  $\text{MeV}^{-1}$  and (8.5, 8.5)  $\text{MeV}^{-1}$  and  $a_f/a_n$  varying between 1.06 and 1.00.

From these observations we assign the values of fission barriers for  $^{171.3}\text{Yb}$  and  $^{169}\text{Tm}$  as  $27.8 \pm 3.0$  MeV and  $29.8 \pm 3.0$  MeV, respectively. The uncertainties shown would allow for inclusion of other values derived from reasonable upper and lower limits of  $a_f$  and  $a_n$  values.

There are several features in the present data which merit comparison with other similar data for low- $Z$  systems. First, it is seen that for erbium (nat) and holmium systems the “best” value of  $a_f$  corresponds to  $A/13$  and  $A/12$ , respectively, whereas Raisbeck and Cobble [8] found  $a_f = A/8$  for thulium and lutetium and a rather anomalously low value of  $A/20$  for rhenium (nat). This was attributed to two possible reasons, the first being due to its proximity to the closed-shell region and the second being due to the use of mixed isotopes. In this context, it might be pointed out that, in the case of erbium (nat) and holmium, there appears to be no such preference for the lower limit of  $a_f = A/20$  in the theoretical fits of the  $\Gamma_f/\Gamma_n$  data (see Figs. 5 and 6). However, since Burnett *et al.* [7] found  $a_f \approx A/11$  for the fission of gold and Brodzinski and Cobble [12] found  $a_f = A/10$  for the fission of natural iridium, which has two isotopes having a similar isotopic abundance as natural rhenium, the reason for the anomaly in the rhenium system still remains not fully understood.

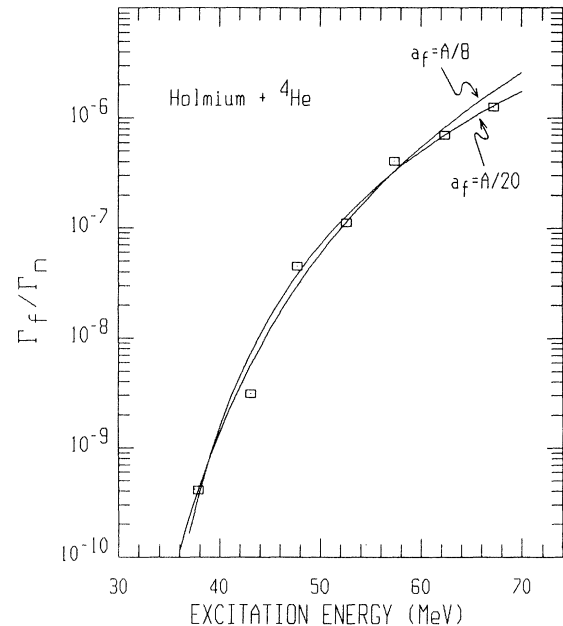


FIG. 5. Theoretical fits to the  $\Gamma_f/\Gamma_n$  data for the He-ion-induced fission of  $^{165}\text{Ho}$  using  $a_f$  values  $A/8$  and  $A/20$ .

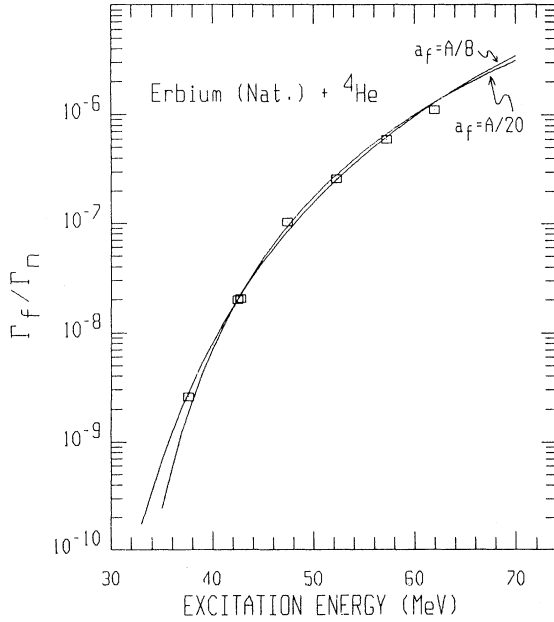


FIG. 6. Theoretical fits to the  $\Gamma_f/\Gamma_n$  data for the He-ion-induced fission of  $^{167.3}\text{Er}$  (nat) using  $a_f$  values  $A/8$  and  $A/20$ .

A systematic trend is observable with regard to the  $a_f/a_n$  values in the lighter element region. As one moves away from the closed-shell region the  $a_f/a_n$  values tend to decrease and reach a value close to unity. The  $a_f/a_n$  values of 1.35, 1.18, 1.17, 1.11, 1.08,  $\sim 1.03$ , and 1.04 for gold [7], iridium [12], rhenium [8], lutetium [8], thulium [8], and erbium, and holmium, respectively, (Tables III and IV) very clearly demonstrate this trend. It may be noted [11] in this context that the ground-state excitation of nuclei in the region of heavy elements (which have a strongly elongated shape in the ground state) exhibit many similarities including the channel spectrum to those of the saddle point. It is possible that the rare-earth nuclei which are also deformed in their ground state exhibit a similar trend which in turn may lead to  $a_f$  and  $a_n$  values which are nearly close to each other.

The experimental fission barriers of  $^{171.3}\text{Yb}$  and  $^{169}\text{Tm}$

measured in this work have been compared with the simple liquid-drop barriers of Cohen and Swiatecki [22] and with shell-corrected values of Myers and Swiatecki [9]. This is illustrated in Fig. 7 where the fissionability parameter  $X$  is given by the ratio  $(Z^2/A)/(Z^2/A)_{\text{critical}}$ , where  $(Z^2/A)_{\text{critical}}$  is taken as 48.5. Measured values of fission barriers of several other low- $Z$  systems to include nuclei closer to as well as away from closed-shell regions (deformed nuclei) are included in Fig. 7 to illustrate the trends [7,8,10,12]. The experimental fission barriers of some of these low- $Z$  nuclides in the deformed and closed-shell regions were also compared with modified liquid-drop models [26–28]. The results are given in Table V. The finite-range models of Sierk [26] and Mustafa *et al.* [27] include finite-range nuclear force and a diffuse nuclear surface. These models differ from that of Cohen-Plasil-Swiatecki [28] in the shape parametrization and in the calculations of the surface, Coulomb, and rotational energies. The calculated barriers of the finite-range models [26,27] are lower than the liquid-drop-model (LDM) barriers for lighter nuclei and are more realistic predictions than that of LDM of Cohen *et al.* [28]. The fission barriers based on Sierk model [26] and LDM of Cohen *et al.* [28] were calculated by ALICE computer code [21] for nonrotating fissioning nuclei. The barriers based on the model of Mustafa *et al.* were read from the graph of  $Z^2/A$  versus fission barrier of beta stable nonrotating fissioning nuclei given in their paper [27]. It is seen that the experimentally measured fission barriers of  $^{171.3}\text{Yb}$  and  $^{169}\text{Tm}$  of  $27.8 \pm 3.0$  and  $29.8 \pm 3.0$  MeV, respectively, as well as those for  $^{173}\text{Lu}$ ,  $^{179}\text{Ta}$ ,  $^{191}\text{Ir}$ , and  $^{189}\text{Ir}$  (Ref. [8]), lie fairly close to the theoretical liquid-drop barrier limit (see Table V and Fig. 7). It implies that the ground-state deformation of these nuclides does not have any observable effect on the fission barrier. Considering the extremely low fission cross sections involved and the difficulties associated with the measurements, the observed general trend is remarkable. Another equally interesting observation is that because of the large ground-state deformation of the nuclides, erbium and holmium (this work), and lutetium, thulium and rhenium (Ref. [8]), the shell corrections to the liquid-drop barrier are relatively small as compared to substantial corrections for nuclides in the gold-bismuth region. This tends to suggest that the basic features of the simple

TABLE III. Least-squares fit of the theoretical  $\Gamma_f/\Gamma_n$  expression to the experimental data on holmium.  $^{165}_{67}\text{Ho} + ^4_2\text{He} \rightarrow ^{169}_{69}\text{Tm}$ .

$E_f$ (MeV)	$a_f$ (MeV $^{-1}$ )	$a_n$ (MeV $^{-1}$ )	$a_f/a_n$	$\psi^2$	Remarks
27.4	21.1	19.9	1.06	0.136	$a_f = A/8$
29.0	16.9	15.9	1.06	0.133	$A/10$
29.2	15.4	14.8	1.04	0.135	$A/11$
29.8	14.1	13.5	1.04	0.127	$A/12$
30.4	13.0	12.5	1.04	0.129	$A/13$
30.8	12.1	11.6	1.04	0.132	$A/14$
30.4	10.6	10.4	1.02	0.134	$A/16$
32.4	9.4	9.2	1.02	0.150	$A/18$
32.6	8.5	8.5	1.00	0.159	$A/20$

TABLE IV. Least-squares fit of the theoretical  $\Gamma_f/\Gamma_n$  expression to the experimental data on erbium (nat).  $^{167.3}_{68}\text{Er} + {}^4_2\text{He} \rightarrow {}^{171.3}_{70}\text{Yb}$ .

$E_f$ (MeV)	$a_f$ (MeV <sup>-1</sup> )	$a_n$ (MeV <sup>-1</sup> )	$a_f/a_n$	$\psi^2$	Remarks
25.0	21.4	20.8	1.03	0.015	$a_f = A/8$
26.2	17.1	16.8	1.02	0.013	$A/10$
26.9	15.6	15.3	1.02	0.011	$A/11$
27.5	14.3	14.0	1.02	0.012	$A/12$
27.8	13.2	13.0	1.01	0.009	$A/13$
28.3	12.2	12.1	1.01	0.010	$A/14$
29.1	10.7	10.7	1.00	0.009	$A/16$
30.0	9.5	9.5	1.00	0.016	$A/18$
30.8	8.6	8.6	1.00	0.032	$A/20$

liquid-drop theory are sufficiently accurate in describing the nuclides in the deformed region.

One final comment is on the dependence of  $\Gamma_f/\Gamma_n$  with  $Z^2/A$  at a given constant excitation energy. This is illustrated in Fig. 8 where  $\log \Gamma_f/\Gamma_n$  is plotted against  $Z^2/A$  for several nuclides all having a constant excitation energy of 40 MeV [8]. It is seen that there is a linear dependence of  $\log \Gamma_f/\Gamma_n$  with  $Z^2/A$  extending over 7–8 orders of magnitude for low- $Z$  compound nuclear systems starting from  $^{169}\text{Tm}$  with a  $\Gamma_f/\Gamma_n$  value of  $< 10^{-9}$  upwards to  $^{213}\text{At}$  with a  $\Gamma_f/\Gamma_n$  value of  $\sim 10^{-2}$  and all of which are characterized by a predominance of sym-

metric fission. The estimated  $\log \Gamma_f/\Gamma_n$  values for the compound nuclei  $^{169}\text{Tm}$  and  $^{171.3}\text{Yb}$  in the present work appear to deviate slightly from the linear relation (Fig. 8). The  $\log \Gamma_f/\Gamma_n$  values of  $-8.96$  and  $-8.2$  for  $^{169}\text{Tm}$  and  $^{171.3}\text{Yb}$ , respectively, from the present work shown in Fig. 8 are estimated by using “best-fit” fission barriers (29.8 MeV for  $^{169}\text{Tm}$  and 27.8 MeV for  $^{171.3}\text{Yb}$ ) based on experimental fission cross sections given in Tables I and II. The deviation of the estimated  $\log \Gamma_f/\Gamma_n$  values for the compound nuclei  $^{169}\text{Tm}$  and  $^{171.3}\text{Yb}$  in the present work from the linear relationship shown in Fig. 8 may be because of the large uncertainties involved in the measure-

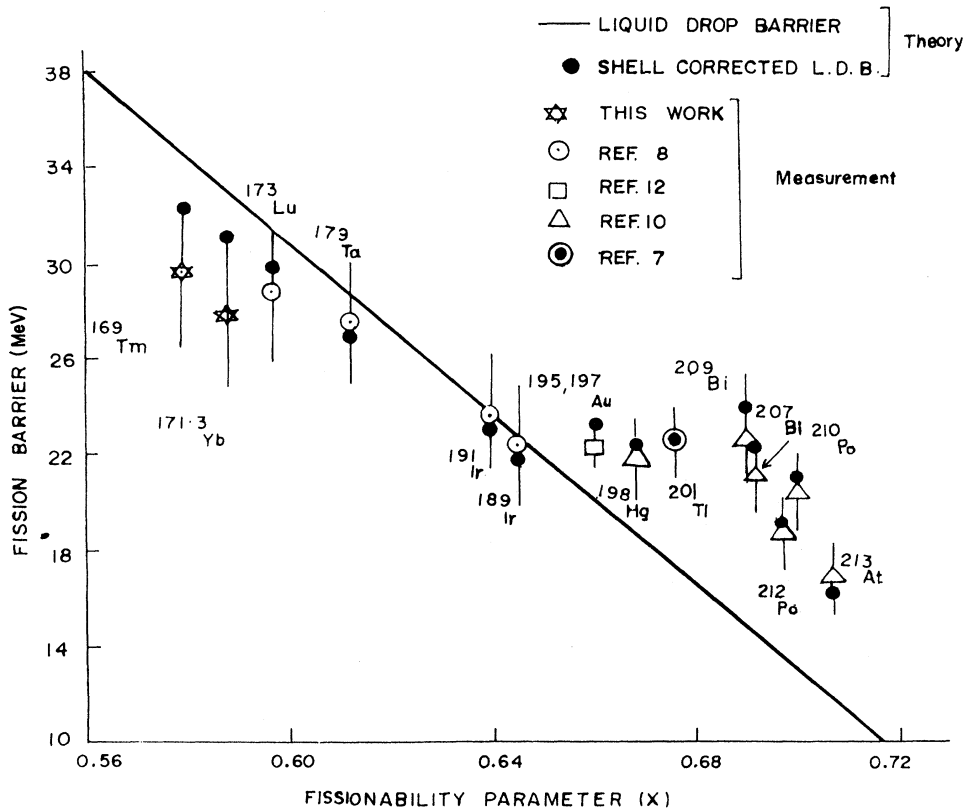


FIG. 7. Comparison of measured and predicted fission barriers for low- $Z$  systems.

TABLE V. Experimental and theoretical fission barriers for some closed shell and deformed shell fissioning nuclei:

Compound Nucleus	Experimental fission barrier (MeV)	Liquid-drop barrier	Liquid-drop barrier	Shell-Corrected L.D. barrier	Finite-range model		Ref.
		(Cohen-Swiatecki) (Ref. [22]) (MeV)	(Cohen <i>et al.</i> ) (Ref. [28]) (MeV)	(Mayers-Swiatecki) (Ref. [9]) (MeV)	Sierk model (Ref. [26]) (MeV)	Mustafa <i>et al.</i> (Ref. [27]) (MeV)	
$^{169}\text{Tm}$	$29.8 \pm 3$	34.6	31.2	32.6	26.6	28.3	This work
$^{171.3}\text{Yb}$	$27.8 \pm 3$	33.1	29.7	31.1	25.3	27.2	This work
$^{173}\text{Lu}$	$28.7 \pm 2.5$	31.5	28.2	29.6	24.2	25.2	[8]
$^{179}\text{Ta}$	$27.5 \pm 2.5$	28.9	25.7	26.8	22.1	23.3	[8]
$^{189}\text{Ir}$	$22.4 \pm 2.5$	22.9	20.0	21.8	17.6	17.8	[8]
$^{191}\text{Ir}$	$23.6 \pm 2.5$	23.5	20.5	23.2	18.0	19.0	[8]
$^{195,197}\text{Au}$	$22.3 \pm 0.7$	20.1	17.6	21.6	15.5	15.9	[12]
		20.7	18.1	23.4	15.9	17.5	
$^{201}\text{Tl}$	$22.5 \pm 1.5$	17.4	15.1	22.4	13.6	14.1	[7]
$^{209}\text{Bi}$	$22.6 \pm 1.5$	15.4	12.9	23.9	11.9	13.1	[10]
$^{210}\text{Po}$	$20.4 \pm 1.5$	13.8	11.8	21.0	10.8	11.1	[10]
$^{213}\text{At}$	$16.8 \pm 1.5$	12.7	10.9	16.2	9.9	10.0	[10]

ments of such low-fission cross sections at lower energies. We have examined the influence of the uncertainties associated with lower-energy fission cross sections on fission barriers and  $\log \Gamma_f / \Gamma_n$  values. If we take the upper and lower limits of fission cross sections of  $^{165}\text{Ho}$  and  $^{167.3}\text{Er}$  at 40 MeV  $^4\text{He}$  laboratory energy (Tables I and II) for fission barrier calculation, then the fission barrier varies

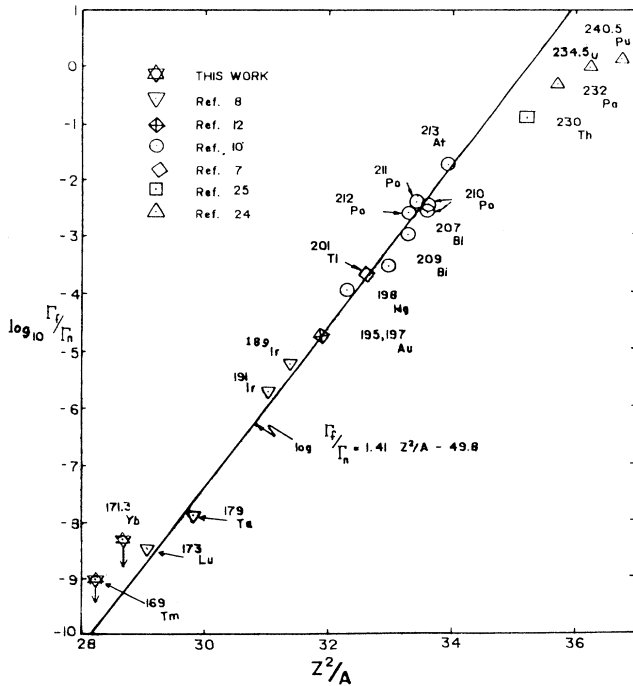


FIG. 8. Correlation of the logarithm of fission to neutron emission width ratios with  $Z^2/A$  at an excitation energy of 40 MeV for different compound nuclei. The logarithms are to the base 10.

from 28.4 to 32.0 MeV for  $^{169}\text{Tm}$  compound nucleus and 27.2 to 30.00 MeV for  $^{171.3}\text{Yb}$  compound nucleus, respectively. Therefore, the uncertainties associated with lower-energy fission cross sections do not affect the “best-fit” barriers ( $29.8 \pm 3$  MeV for  $^{169}\text{Tm}$ ,  $27.8 \pm 3$  MeV for  $^{171.3}\text{Yb}$ ) obtained by using the experimental fission cross-section values given in Tables I and II. However, the estimated  $\log \Gamma_f / \Gamma_n$  values at 40 MeV excitation energy vary between  $-10.1$  and  $-8.2$  for  $^{169}\text{Tm}$  and between  $-9.1$  and  $-7.8$  for  $^{171.3}\text{Yb}$  if we take the upper and lower limits of the fission barriers ( $32.0$  to  $28.4$  for  $^{169}\text{Tm}$  and  $30.0$  to  $27.2$  MeV for  $^{171.3}\text{Yb}$ , which in turn were obtained by using the lower and upper limits of the lowest-energy cross sections, respectively). The expected  $\log \Gamma_f / \Gamma_n$  value from the linear relationship (Fig. 8) is  $-10.08$  for  $^{169}\text{Tm}$  and  $-9.47$  for  $^{171.3}\text{Yb}$ . The estimated  $\log \Gamma_f / \Gamma_n$  values of  $-8.96$  and  $-8.20$  (Fig. 8) based on the “best-fit” fission barriers lie within the calculated limits of  $-10.1$  and  $-8.2$  for  $^{169}\text{Tm}$  and  $-9.1$  and  $-7.8$  for  $^{171.3}\text{Yb}$  respectively. Therefore, we believe that the small deviation of the  $\log \Gamma_f / \Gamma_n$  values for  $^{169}\text{Tm}$  and  $^{171.3}\text{Yb}$  from the linear trend is not real. Any true deviation would mean a lower fission barrier (enhanced fissionability). In fact, the data given in Fig. 7 do not bear out this possibility. The linear dependence starts deviating at about  $^{230}\text{Th}$  ( $^{226}\text{Ra} + ^4\text{He}$ ), which is the region where symmetric and asymmetric fission was observed to occur in comparable amounts [4]. The two fission modes [23] are probably competing in all cases but are dependent on different parameters and therefore one may mask the other [29]. The recent extremely difficult and careful study of Itkis *et al.* [30] on symmetric and asymmetric fission of nuclei lighter than thorium indicates that asymmetry of mass distribution is present well below the Ra region and disappears somewhat abruptly near  $A = 200$ . It may be argued that there is no appreciable effect of asymmetric fission on the linear dependency of  $\log \Gamma_f / \Gamma_n$  on  $Z^2/A$  below  $^{213}\text{At}$  because of the very small contribution



of asymmetric fission, but the linear dependency start deviating at about  $^{230}\text{Th}$  where contributions from asymmetric fission becomes significant. In fact, many characteristics of fission (barriers, probability of fission, and mass distributions of fission fragments) are strongly dependent on the nucleon composition of fissioning nuclei, being substantially different from the features predicted by the liquid-drop model. Their origin is associated with the shell structure of the potential energy of the nuclear deformation which provides a theoretical basis [29] for the "two-mode" fission hypothesis of Turkevich and Niday [23]. The most drastic changes take place in the transition from the preactinides to actinides. The nuclei lighter than Ra undergo mainly symmetric fission (with small contributions of asymmetric fission—Itkis *et al.* [30]) and characterized by a sharp increase of the barrier heights and by a decrease of the fissility with a de-

crease in  $Z^2/A$ . On the other hand, the actinide nuclei undergo predominantly asymmetric fission with a relatively weak dependence of the fission barriers and fissility on  $Z^2/A$ .

At present, our efforts are continuing to extend these measurements to ytterbium ( $Z=70$ ) and terbium ( $Z=65$ ) and also to use separated erbium isotopes.

#### ACKNOWLEDGMENTS

We appreciate the help and cooperation extended to us by Dr. S. N. Chintalapudi, Dr. R. K. Bhandari, V. S. Pandit, and the operating staff of the Variable Energy Cyclotron (VEC), Calcutta, in carrying out the cyclotron irradiations. We also thank Dr. S. K. Saha of VEC, Calcutta for his help during these experiments.

- 
- [1] E. K. Hyde, *Nuclear Properties of Heavy Elements*, Vol. III of *Fission Phenomena* (Prentice-Hall, Englewood Cliffs, 1964).
- [2] R. Vandenbosch and J. R. Huizenga, *Nuclear Fission* (Academic, New York, 1973).
- [3] A. W. Fairhall, *Phys. Rev.* **102**, 1335 (1956).
- [4] A. W. Fairhall, R. C. Jensen, and F. E. Neuzil, *Proceedings of the Second United Nations Conference on the Peaceful Uses of Atomic Energy*, Geneva, 1957 (United Nations, New York, 1958), paper P/677, Vol. 15.
- [5] J. R. Huizenga, R. Chaudhry, and R. Vandenbosch, *Phys. Rev.* **126**, 210 (1962).
- [6] R. L. Fleischer, P. B. Price, and R. M. Walker, *Nuclear Tracks in Solids: Principle and Application* (University of California Press, Berkeley, 1975).
- [7] D. S. Burnett, R. C. Gatti, F. Plazil, P. B. Price, W. J. Swiatecki, and S. G. Thompson, *Phys. Rev.* **134**, B952 (1964).
- [8] G. M. Raisbeck and J. W. Cobble, *Phys. Rev.* **153**, 1270 (1967).
- [9] W. D. Myers and W. J. Swiatecki, Lawrence Radiation Laboratory Report No. UCRL/11980, 1965.
- [10] A. Khodai-Joopari, University of California Radiation Laboratory, Report No. UCRL-16489, 1966.
- [11] A. Bohr, *Proceedings of the First United Nations Conference on the Peaceful Uses of Atomic Energy*, Geneva, 1955. (United Nations, New York, 1956), paper P/911. Vol. 2.
- [12] R. L. Brodzinski and J. W. Cobble, *Phys. Rev.* **172**, 1194 (1968).
- [13] K. G. Kuvatov, V. N. Okolovich, L. A. Smirina, G. N. Smirenkin, V. P. Bochinn, and V. S. Romanov, *Yad. Fiz.* **14**, 79 (1971) [*Sov. J. Nucl. Phys.* **14**, 45 (1972)].
- [14] P. C. Kalsi, R. C. Sharma, A. K. Pandey, and R. H. Iyer, *Proceedings of the DAE Symposium on Radiochemistry and Radiation Chemistry*, Indira Gandhi Centre for Atomic Research (IGCAR), Kalpakkam, India, Jan. 4–7, 1989, paper R-1.
- [15] R. H. Iyer, P. C. Kalsi, A. K. Pandey, and R. C. Sharma, *Proceedings of the DAE Symposium on Nuclear Physics*, Aligarh Muslim University, Aligarh, India, Dec. 26–30, 1989, paper O-38.
- [16] K. A. Kraus and F. Nelson, *Proceedings of the First United Nations Conference on the Peaceful Uses of Atomic Energy*, Geneva, 1955 (United Nations, New York, 1956), paper P/837, Vol. 7, p. 113.
- [17] Obtained from General Electric Corporation, Pittsfield, Ma.
- [18] S. Bjornholm, P. H. Dam, H. Nordby, and N. O. Roy Poulson, *Nucl. Instrum. Methods* **5**, 196 (1959).
- [19] N. K. Choudhuri, V. Natarajan, R. Sampath Kumar, M. L. Sagu, and R. H. Iyer, *Nucl. Tracks* **3**, 69 (1979).
- [20] J. R. Huizenga and G. J. Igo, *Nucl. Phys.* **29**, 462 (1962).
- [21] M. Blann, LLNL Report No. UCID 19614, 1982.
- [22] S. Cohen and W. J. Swiatecki, *Ann. Phys. (N.Y.)* **22**, 406 (1963).
- [23] A. Turkevich and J. B. Niday, *Phys. Rev.* **84**, 52 (1951).
- [24] R. Vandenbosch and J. R. Huizenga, *Proceedings of the Second United Nations Conference on the Peaceful Uses of Atomic Energy*, Geneva, 1957 (United Nations, New York, 1958), paper P/688, Vol. 15.
- [25] J. E. Gindler, G. L. Bate, and J. R. Huizenga, *Phys. Rev.* **136**, B1333 (1964).
- [26] A. J. Sierk, *Phys. Rev. C* **33**, 2039 (1986).
- [27] M. G. Mustafa, P. A. Baisden, and H. Chandra, *Phys. Rev. C* **25**, 2524 (1982).
- [28] S. Cohen, F. Plasil, and W. J. Swiatecki, *Ann. Phys.* **82**, 557 (1974).
- [29] V. V. Pashkevich, *Nucl. Phys.* **A169**, 275 (1971).
- [30] M. G. Itkis, V. N. Okolovich, A. Ya. Rusanov, and G. N. Smirenkin, *Fiz. Elem. Chastits At. Yadra* **19**, 701 (1988) [*Sov. J. Part. Nucl.* **19**, 301 (1988)].

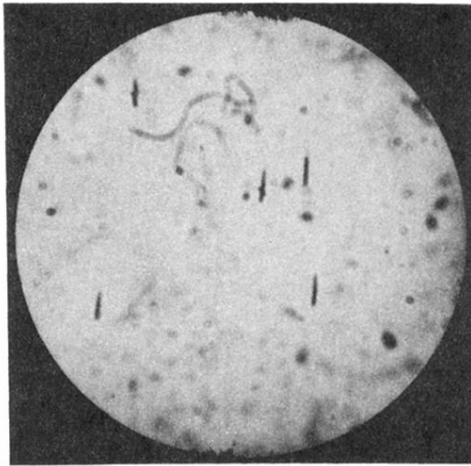


FIG. 2. Photomicrograph of the oriented fission fragment tracks in lexan from the 65 MeV He-ion-induced fission of  $^{165}\text{Ho}$ .